Synthesis of Photoisomerizable Block Copolymers by Atom Transfer Radical Polymerization

Chih-Feng Huang, Wei Chen, Thomas P. Russell, Anna C. Balazs, Feng-Chih Chang, Krzysztof Matyjaszewski*

A series of polystyrene-*block*-poly(*n*-butyl methacrylate) (PS-*b*-P*n*BMA) diblock copolymers (di-BCPs) with an azobenzene moiety [*trans*-4-methacryloyloxyazobenzene (MOAB)] in the P*n*BMA segment was prepared by atom transfer radical polymerization (ATRP). P(*n*BMA-*co*-MOAB) macroinitiators were prepared by activators regenerated by electron transfer (ARGET) ATRP. The MOAB was slightly more reactive than *n*BMA, resulting in a weak gradient fashion of copolymer. The macroinitiators were subsequently chain-extended with styrene. Acceleration of the ATRP rate was observed in the presence of a reducing agent. P(*n*BMA-*co*-MOAB)-*b*-PS di-BCPs were obtained with relatively narrow molecular weight distributions ($\overline{M}_w/\overline{M}_n = 1.16–1.49$) and the molecular weights were in good agreement with the theoretical values. The efficiency of photoisomerization of the MOAB units was above 80%. DSC traces showed a single T_g suggesting the block copolymers were miscible before UV irradiation. After UV irradiation, the X-ray reflectivity measurements showed the beating of two frequencies, indicating the formation of island-hole structure.

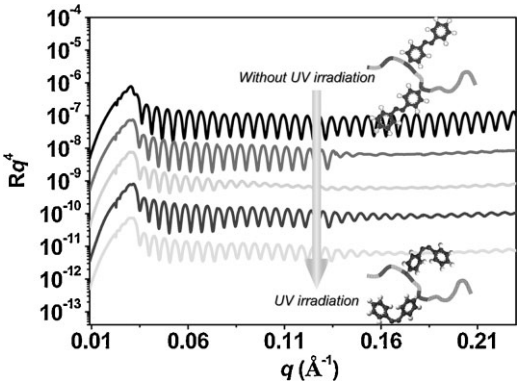

Introduction

Block copolymers (BCPs) are self-assembling systems, in which chemically distinct blocks microphase separate into nanoscale periodic domains, comprising lamellar, cylindrical, and body centered cubic spherical structures, depending on the solubility parameter and the relative volume fractions of the blocks.[1,2] During heating, the translational entropy increases and segmental interactions usually decrease; therefore a transition from a phase-separated to a phase-mixed state is expected. This happens at upper order-to-disorder transition (UODT) for BCPs, or the upper critical solution transition (UCST) for polymer mixtures and is accompanied by a small volume change on mixing.[3,4] BCPs and polymer mixtures can also undergo a transition from the phase-mixed to phase separated state on heating.

C.-F. Huang, K. Matyjaszewski
Department of Chemistry, Carnegie Mellon University, 4400 Fifth Avenue, Pittsburgh, Pennsylvania, PA 15213, USA
Fax: (+1) 412 268 6897; E-mail: km3b@andrew.cmu.edu
W. Chen, T. P. Russell
Department of Polymer Science and Engineering, University of Massachusetts, Amherst, Massachusetts, MA 01003, USA
A. C. Balazs
Department of Chemical Engineering, University of Pittsburgh, Pittsburgh, PA 15261, USA
C.-F. Huang, F.-C. Chang
Department of Applied Chemistry, National Chiao Tung University, Hsinchu 30050, Taiwan

Macromol. Chem. Phys. **2009**, *210*, 1484–1492

DOI: 10.1002/macp.200900195

This is referred to as the lower disorder-to-order transition (LDOT) for BCPs or the lower critical solution transition (LCST) for polymer mixtures. The difference in thermal expansion coefficients of two segments increases with increase in temperature; when this effect dominates over the reduction in the enthalpic repulsive energy, LDOT (or LCST) occurs accompanied by a positive volume change on demixing.[5,6] Russell and coworkers[7–13] studied the phase behavior of a series of polystyrene-*block*-poly(*n*-alkyl methacrylate) BCPs and blends by rheological measurements, small angle X-ray scattering (SAXS), and small angle neutron scattering (SANS). They summarized the results of phase behavior of these diblock copolymers (di-BCPs), i.e., the type of behavior (UODT vs. LDOT) and transition temperatures for each system. The value of solubility parameter (δ) for the methacrylates monotonically decreased with increase in alkyl side chain length. The value for polystyrene (PS) was closest to that of poly(*n*-butyl methacrylate) (P*n*BMA). This qualitatively supports the observation of a minimum in δ, between the styrene and the *n*BMA block for intermediate side chain lengths. The main thermodynamic trend for this family of materials was successfully established.

Phase transition can be induced not only by temperature but also by pressure[14–16] and light. BCPs containing photo-addressable side groups have the possibility to create hierarchically ordered materials that are defect-free on relatively large length scales. This analog of photo-addressable molecules include photo-responsive molecules that photo-dimerized, such as coumarins and anthracenes; those that allow intra-molecular photo-induced bond formation, such as spiropyrans, and diarylethenes; and those that exhibit photo-isomerization, such as stilbenes, crowded alkenes, and azobenzenes.[17] Tran-Cong-Miyata and coworkers[18–21] demonstrated the concept of photo-tuning microphase separated structures in polymer mixtures for a series of *trans*-stilbene labeled PS and poly(vinyl methyl ether) (PSS/PVME) blends. Upon irradiation, the stilbene moieties on the PSS chains begin to undergo a reversible *trans-cis* photoisomerization. When the reaction surpasses a certain threshold, the mixture undergoes phase separation, since the *cis*-labeled PS and the PSS/PVME are immiscible. Phase separation and a reversible chemical reaction are taking place simultaneously within this binary blend. Furthermore, Balazs and coworkers[22,23] presented computational models to demonstrate a promising photo-rastering method which resulted in the formation of defect-free, spatial periodic structures. Among the photo-tunable molecules, azobenzene is a promising candidate to mimic this strong photo-switching effect with respect to reversibility, speed, and simplicity of incorporation.[17,24–27] The phase behavior of these functional groups in polymer mixtures and BCPs has been studied extensively. Reversible photochemical reactions induced phase separation in a BCP system has been recently reported. Iyoda and coworkers[28,29] utilized ATRP to synthesize a series of liquid crystalline homopolymers and amphiphilic di-BCPs with PEO as the hydrophilic block and a polymethacrylate with azobenzene unit as the hydrophobic and photoactive part, respectively. They further demonstrated a parallel patterning of PEO nanocylinders in the film of an amphiphilic di-BCP consisting of a polymethacrylate block with an azobenzene unit, using a linearly polarized laser beam (488 nm). The PEO nanocylinders were aligned normal to the polarization direction of the light.[30,31] One of the most promising examples, from Seki and coworkers[32], uses ATRP to develop an ABA-type triblock copolymer (tri-BCP) where A and B correspond to azobenzene-containing polymethacrylate and PEO, respectively. The morphology of a monolayer film of the tri-BCP (*trans* form) on a mica substrate showed nanoscopic dot and rod features. After UV irradiation, the film presented striped features. Thermal *cis-trans* isomerization at room temperature caused the stripes to revert to dots.

Photoinduced isomerization can result in conformational change, if the azobenzene or stilbene unit is incorporated in the main or side chain. These photoinduced changes can be reversed by heat or visible irradiation. It is important to understand critical relationship between the photo-addressable composition in polymer chain and the physical property changes, such as the solubility parameter, morphology, or refractive index. This study is focused on syntheses and characterization of and PS-*b*-P*n*BMA BCP with azobenzene moiety (*trans*-4-methacryloyloxy azobenzene, MOAB) in the P*n*BMA segment. BCPs were prepared by atom transfer radical polymerization (ATRP).[33–35] In the first step activators regenerated by electron transfer (ARGET) ATRP was used to prepare poly[(*n*-butyl methacrylate)-*co*-(*trans*-4-methacryloyloxyazobenzene)] [P(*n*BMA-*co*-MOAB)] macroinitiators (MI).[36–40] The MIs were subsequently chain-extended with styrene to form P(*n*BMA-*co*-MOAB)-*b*-PS di-BCPs with relatively narrow molecular weight distributions (1.16–1.49) and the molar masses in good agreement with the theoretical values. The aim of this work is to adjust the LDOT behavior of the BCP by UV–Vis irradiation. In this paper we describe synthesis of a series of BCPs with different molecular weights, different azobenzene content, and discuss their basic thermo- and photochemistry. Subsequently, their phase behavior will be reported.

Experimental Part

Materials

n-Butyl methacrylate (*n*BMA, 99%), and styrene (S, 99%), were purchased from Aldrich and purified by passing through a column filled with basic alumina to remove the inhibitors or antioxidants.

4-Hydroxyazobenzene (98%), ethyl 2-bromoisobutyrate (EBiB, 98%), methacryloyl chloride (97%), triethylamine (98%), *N,N,N′,N″,N″*-pentamethyldiethylenetriamine (PMDETA, 99%), and tin(II) 2-ethylhexanoate ($Sn(EH)_2$, 99%) were purchased from Aldrich and were used without further purification. Tris[2-(dimethylamino)ethyl]amine (Me_6TREN) was synthesized according to the literature.[41] Copper(I) bromide (CuBr, 98%, Acros) was washed with glacial acetic acid in order to remove any soluble oxidized species, filtered, washed with ethanol, and dried. All solvents were purified by distillation prior to use.

Synthesis of *trans*-4-Methacryloyloxyazobenzene

Trans-4-methacryloyloxyazobenzene was synthesized according to the literature.[42,43] 4-Hydroxyazobenzene (10 mmol) was dissolved in 20 mL of dry THF, after which triethylamine (10.6 mmol) and 1 mg of inhibitor were added to the solution. Methacryloyl chloride (30 mmol) was added gradually to the solution while the flask was cooled in an ice-cooled water bath. The triethylammonium salt started to accumulate immediately after the addition of methacryloyl chloride. The reaction mixture was stirred for 30 h. At the end of the reaction, the organic layer was washed and the yellow organic layer was dried. The resulting yellow solid was purified by passing a chloroform solution through a silica column. The product was crystallized twice from hexane. A yield of 62% was obtained. ^{1}H NMR ($CDCl_3$): $\delta = 8.05$–7.25 (m, aromatic, 9H); 6.4-5.79 (s, double bond, 2H); 2.1 (s, methyl, 3H).

Preparation of Macroinitiator Using Activators Regenerated by Electron Transfer Atom Transfer Radical Polymerization for the Copolymerizations of *n*-Butyl Methacrylate and *trans*-4-Methacryloyloxy Azobenzene

The initiator, ethyl 2-bromoisobutyrate (EBiB) (0.041 mmol) and copper(I) bromide complex (100 ppm to monomer)/tris(2-(dimethylamino)ethyl)amine ([CuBr]/[Me_6TREN] = 0.3:1) were added to a Schlenk flask. Nitrogen-purged *n*BMA (12.2 mmol) and various amount of MOAB monomer were added, followed by addition of anisole ([*n*BMA]$_0$ = 3.13 M). $Sn(EH)_2$ (10 fold excess over CuBr) was added and stirred for 15 min to form a homogeneous mixture. The flask was then transferred to a 60 °C oil bath. Samples were removed at different time intervals during polymerization, and conversion and molecular weights were determined by GC and GPC. The polymerization was stopped at the desired conversion ($\overline{M}_n$) by exposing the reaction to air.

Block Copolymerization of Styrene from Poly[(*n*-butyl methacrylate)-*co*-(*trans*-4-methacryloyloxy azobenzene)] Macroinitiator Using Atom Transfer Radical Polymerization

In the sequential step of block copolymerization (Scheme 1), well-defined P(*n*BMA-*co*-MOAB)-*b*-PS was synthesized by ATRP with PMDETA ligand. Typically, the ratio of reagents was [S]$_0$/[MI]$_0$/[CuBr]$_0$/[PMDETA]$_0$/[$Sn(EH)_2$]$_0$ equal to 700:1:1:1:1 in anisole solution ([S]$_0$ = 4.35 M). Styrene, PMDETA, MI, and anisole were added to a 25 mL Schlenk flask. The resulting mixture was deoxygenated by three freeze-pump-thaw cycles. The reaction flask was filled with nitrogen, and then CuBr was added to the frozen solution. The flask was closed, evacuated with a vacuum, and deoxygenated by two freeze-pump-thaw cycles. An initial sample was taken via a syringe and the flask was then immersed in an oil bath preheated at 90 °C to start the polymerization. Aliquots were withdrawn at different time intervals during the polymerization to monitor the conversion by GC. The polymerization was stopped at desired conversion. The resulting mixture was diluted with THF and filtered through a neutral aluminum oxide column to remove the copper catalyst and dried in vacuum to a constant mass.

Measurements

Proton Nuclear Magnetic Resonance (^{1}H NMR) spectra were recorded on a Bruker instrument operating at 300 MHz in deuterated chloroform at 30 °C. Conversions of volatile monomers were determined by a Shimadzu GC 14-A gas chromatograph equipped with a FID detector using a J&W Scientific 30 m WAX

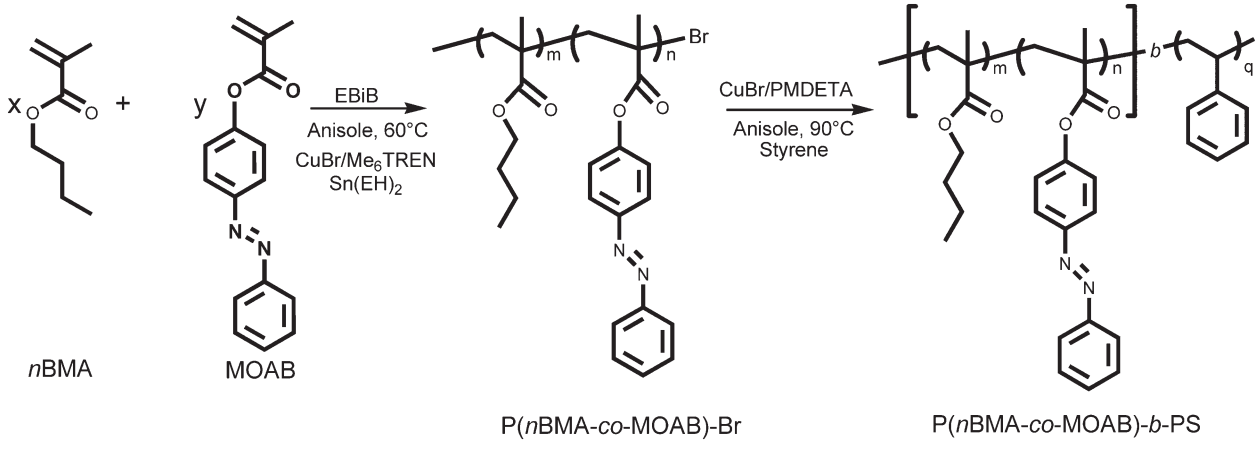

Scheme 1. Synthetic route to prepare photoisomerizable di-BCPs.

Macromol. Chem. Phys. **2009**, *210*, 1484–1492

Macromolecular Journals

DOI: 10.1002/macp.200900195

Megabore column and anisole as internal standard. Apparent molecular weight and molecular weight distributions were measured on a GPC system consisting of a Waters 510 HPLC pump, three Waters UltraStyragel columns (10^2, 10^3, and 10^5 Å), and a Waters 410 differential refractive index detector, with a THF flow rate of 1.0 mL · min^{-1} and PS as standards.

To investigate the effects of UV and visible light irradiation, a high power mercury arc lamp (200 W), covering range from UV to visible light was used. The intensity was 50 mW · cm^{-2} after passing through a wavelength filter and IR block filter. 365 and 440 nm wavelength filters were used for UV and visible light irradiation, respectively. UV–Vis spectra were recorded using a Cary 50 Bio UV–Vis spectrophotometer equipped with a digital temperature controller. Thermal analysis was carried out on a DSC instrument (DuPont model 910 DSC-9000 Controller) with a scan rate of 20 °C · min^{-1} and temperature range of 0–200 °C under a nitrogen atmosphere. The samples (ca. 5–10 mg) were sealed in an aluminum pan. The samples were cooled rapidly to room temperature from the first scan and then up to 180 °C at a scan rate of 20 °C · min^{-1}. The glass transition temperature was recorded as the midpoint of the heat capacity transition between the upper and lower points of deviation from the extrapolated glass and liquid lines.

Results and Discussion

Copolymerizations of *n*-Butyl Methacrylate and *trans*-4-Methacryloyloxy Azobenzene

The P(*n*BMA-*co*-MOAB)-*b*-PS block copolymers (BCPs) were synthesized starting from the methacrylate block using ARGET ATRP for the first step (Scheme 1).

The conversion for each monomer was measured by ^{1}H NMR. The kinetic plots are shown in Figure 1. The faster monomer consumption of the MOAB monomer (squares) indicated its higher reactivity than the *n*BMA monomer (diamonds). The total conversion (circles) was equal to $conv._{nBMA} \times 0.9 + conv._{MOAB} \times 0.1$. The apparent rate constant (k_{app}) of MOAB consumption was about two times higher than that of *n*BMA. The higher reactivity of MOAB results in the gradient structure of a copolymer with a higher fraction of MOAB at the initial chain end.

The evolution of molecular weight relative in time is shown in Figure 2. The molecular weight increased linearly with conversion and polydispersity decreased with conversion (PDI < 1.2). This indicated the polymerization system was controlled and a high molecular weight MI was obtained.

The copolymerization was also studied with various azobenzene contents 20, 10, and 5 mol% in feed ratio. All ARGET ATRP copolymerizations showed similar rates, which indicated the amount of azobenzene had no significant influence on the rate and ATRP equilibrium. These observations supported a controlled polymerization system using ARGET ATRP. Table 1 summarizes the characteristics of these P(*n*BMA-*co*-MOAB)-Br copolymers (no. C0–C6).

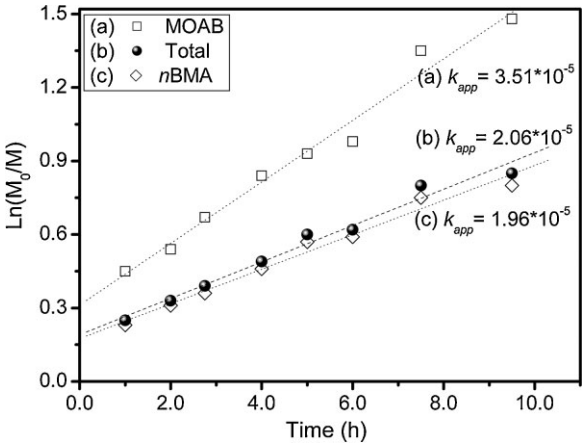

Figure 1. First-order kinetic plot for P(*n*BMA-*co*-MOAB) MI copolymerization (C-6, *n*BMA/MOAB = 90:10) via ARGET ATRP from ^{1}H NMR ([*n*BMA + MOAB]$_o$/[EBiB]$_o$/[CuBr]$_o$/[Me$_6$TREN]$_o$/[Sn(EH)$_2$]$_o$ = 400:1:0.03:0.1:0.3 at 60 °C in 50 vol.-% anisole).

To understand the sequence distribution of each monomer, the reactivity ratios in the P(*n*BMA-*co*-MOAB) copolymer system were also estimated. The reactivity ratio of copolymerization was determined by employing the Kelen–Tüdos method. This method derives the reactivity ratio from the "copolymerization equation" which contains two parameters, η and ξ, as described in previous studies.[44] Figure 3 shows the Kelen–Tüdos plot for P(*n*BMA-*co*-MOAB) copolymers. After estimation with various monomer feed ratio at low conversion, the reactivity ratios for *n*-butyl methacrylate ($r_{nBMA} = 0.9$) and for *trans*-4-methacryloyloxyazobenzene ($r_{MOAB} = 2.29$) were obtained. MOAB showed

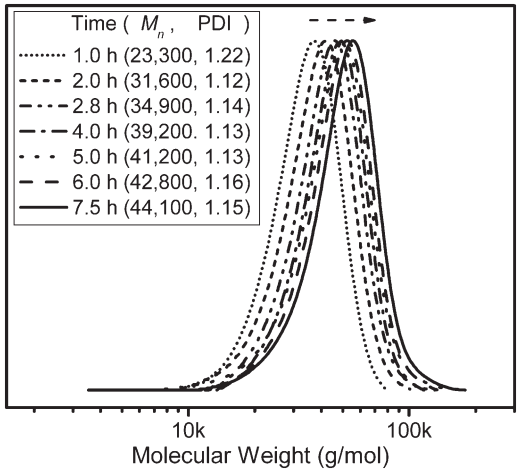

Figure 2. Molecular weight evolution and PDI of P(*n*BMA-*co*-MOAB) copolymerization by GPC analysis (C-6, *n*BMA/MOAB = 90:10) via ARGET ATRP: ([*n*BMA + MOAB]$_o$/[EBiB]$_o$/[CuBr]$_o$/[Me$_6$TREN]$_o$/[Sn(EH)$_2$]$_o$ = 400:1:0.03:0.1:0.3 at 60 °C in 50 vol.-% anisole).

Table 1. Conditions of *n*BMA and MOAB copolymerizations using ARGET ATRP and copolymer characterization.

No.	$[M]_0/[I]_0$[a)]	Time	Conv.	$\overline{M}_n$	PDI	*n*BMA[c)]	MOAB[c)]
	Feed ratios	h	%[b)]	g · mol^{-1}		mol-%	mol-%
C-0	300 (85*n*BMA/15MOAB)	3.8	40.3	26 900	1.21	80.1	19.9
C-1	300 (80*n*BMA/20MOAB)	4.0	44.3	25 900	1.20	72.9	27.1
C-2	300 (90*n*BMA/10MOAB)	2.7	34.4	27 700	1.20	87.0	13.0
C-3	300 (95*n*BMA/05MOAB)	4.5	43.5	26 000	1.16	94.5	5.5
C-4	450 (75*n*BMA/25MOAB)	4.0	47.7	32 000	1.16	71.2	28.8
C-5	150 (75*n*BMA/25MOAB)	3.5	50.3	20 100	1.19	70.5	29.5
C-6	400 (90*n*BMA/10MOAB)	9.5	49.4	46 000	1.14	86.5	13.5

[a)] $[n\text{BMA} + \text{MOAB}]_0/[\text{ethyl 2-bromoisobutyrate}]_0/[\text{CuBr}]_0/[\text{Me}_6\text{TREN}]_0/[\text{Sn(EH)}_2]_0 = (150\text{–}450)/1/0.03/0.1/0.3$, [*n*BMA]/[MOAB] molar ratio in feed of copolymerizations; all at 60 °C in 50 vol.-% anisole except C-2 and C-3 in 33 vol.-% anisole; [b)] Conversion of *n*BMA determined by GC; [c)] Molar percentages were calculated by ^{1}H NMR.

a higher reactivity than *n*BMA during ARGET ATRP, which was in agreement with free radical copolymerizations,[45–47] as also observed in other systems.[48–53] Thus, a weak gradient structure was obtained within the copolymer chain.

Block Copolymerization of Styrene

The P(*n*BMA-*co*-MOAB) copolymers were employed as MIs for ATRP block polymerization of styrene at 90 °C in anisole (50 vol.-%). The chain extension of styrene from P(*n*BMA-*co*-MOAB)-Br MI was slow under typical ATRP conditions, therefore a reducing agent was added to increase the polymerization rate. The apparent rate constants (k_{app}) for the polymerization with and without reducing agent were determined to be 1.25×10^{-5} and 1.1×10^{-6} s^{-1}, respectively (Figure 4). The presence of reducing agent increases the ratio of $[Cu^I]/[Cu^{II}]$ at the equilibrium state in Equation (1) and (2), resulting in the increased R_p.

$$\text{Ln}\left(\frac{[M]_0}{[M]}\right) = k_p K_{eq}[RX]\frac{[Cu^I]}{[Cu^{II}]} \times t \quad (1)$$

$$R_p = k_p[M][P\cdot] = k_p[M]K_{eq}[I]_0\frac{[Cu^I]}{[Cu^{II}]} = k_{app} \times t \quad (2)$$

Figure 5 shows the evolution of molecular weights and PDIs with conversion and GPC traces, for the chain extension from MI C-1. A low polydispersity P(*n*BMA-*co*-MOAB)-*b*-PS di-BCP was formed via ATRP in the presence of reducing agent (Figure 4 line a). The molar masses increased linearly with conversion (Figure 4 line b). They were in good

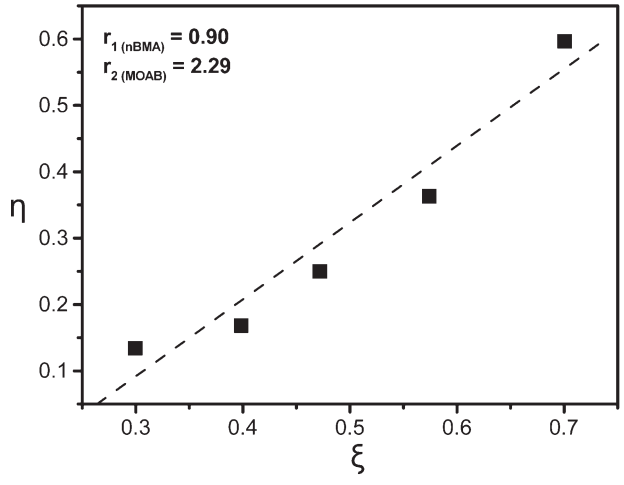

Figure 3. Kelen–Tüdos plot for P(*n*BMA-*co*-MOAB) copolymerizations of C-o–C-4.

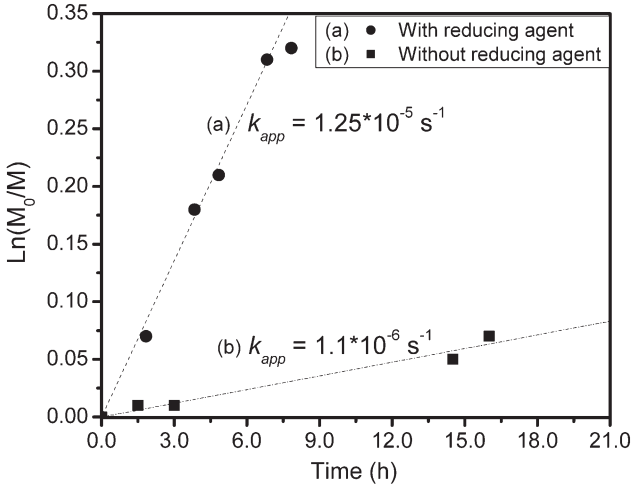

Figure 4. Kinetic plot of P(*n*BMA-*co*-MOAB)-Br MI (C-2) for styrene chain extension by ATRP with (BC-8a) or without (BC-8b) reducing agent at 90 °C in anisole 50 vol.-% $([S]_o/[C\text{-}2]_o/[CuBr]_o/[PMDETA]_o/[Sn(EH)_2]_o = 700{:}1{:}1{:}1{:}1)$.

Macromol. Chem. Phys. **2009**, *210*, 1484–1492

Macromolecular Journals
DOI: 10.1002/macp.200900195

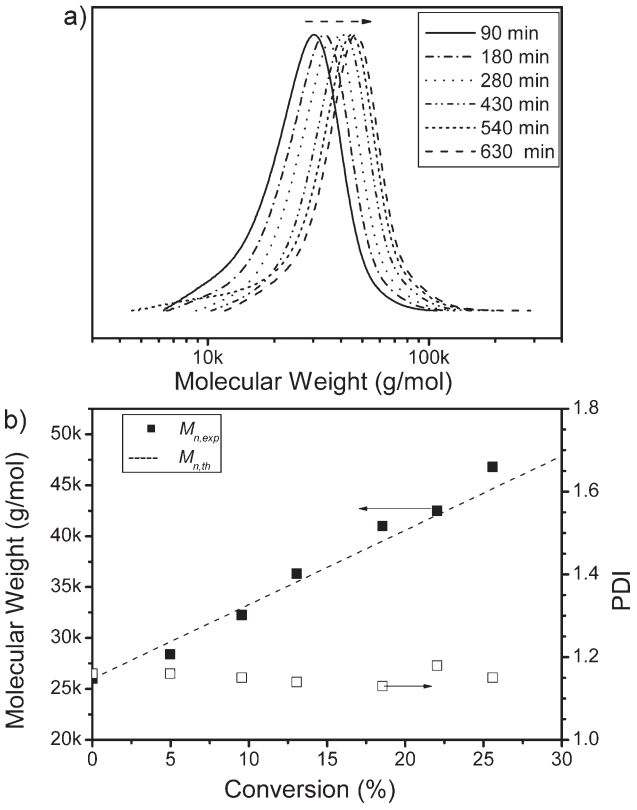

Figure 5. Molecular weight plots for ATRP of styrene from P(*n*BMA-*co*-MOAB)-Br MI C-1 to BC-7: (a) Evolution of molecular weight from GPC traces with PS standard, (b) $\overline{M}_n$ and PDI versus styrene conversion (BC-7: $[S]_0/[C\text{-}1]_0/[CuBr]_0/[PMDETA]_0/[Sn(EH)_2]_0 = 700{:}1{:}1{:}1{:}1$ at 90 °C in 50 vol.-% anisole).

agreement with the calculated values ($\overline{M}_{n,th} = [M]_0/[I]_0 \times$ conversion(%) $\times \overline{M}_{w,Styrene} + \overline{M}_{w,MI}$), and the polydispersity indices were in the range of 1.10–1.25. This showed that a well-controlled block copolymerization of styrene was achieved. The composition of the BCPs were confirmed

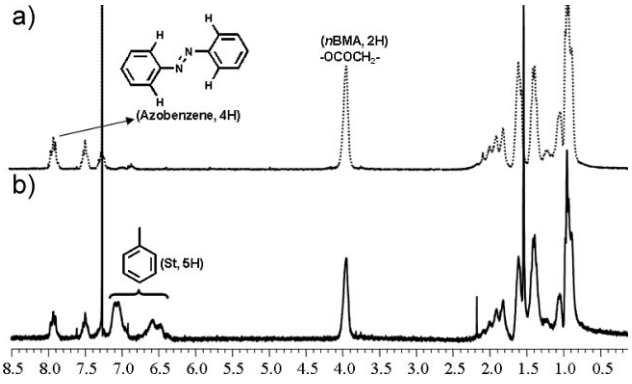

Figure 6. ^{1}H NMR of (a) P(*n*BMA-*co*-MOAB) MI (C-2), and (b) P(*n*BMA-*co*-MOAB)-*b*-PS di-BCP (BC-8a) (BC-8a: $[S]_0/[MI]_0/[CuBr]_0/[PMDETA]_0/[Sn(EH)_2]_0 = 700{:}1{:}1{:}1{:}1$ at 90 °C in 50 vol.-% anisole).

by ^{1}H NMR in $CDCl_3$, which can also determine the molar ratio of each monomer in the MI [Figure 6 Figure 6(a), P(*n*BMA-*co*-MOAB)-Br] and di-BCP [Figure 6(b), P(*n*BMA-*co*-MOAB)-*b*-PS]. The results of the block copolymerization are summarized in Table 2 (no. BC-7–BC-12).

Photochemical and Phase Behavior Measurements

Photoisomerization was carried out in $CHCl_3$ for the series of P(*n*BMA-*co*-MOAB)-*b*-PS BCPs with pendant azobenzene groups, which are listed in Table 2 (samples BC-7–BC-9). Upon irradiation with UV light at 360 nm, the absorption band at around 325 nm decreases significantly, while the band at around 435 nm increases slightly, Figure 7(a)–(c). The absorption bands at 325 and 435 nm are ascribed to π–π^* and n–π^* transitions, respectively; the isosbestic point is around 400 nm. When irradiated by visible light (or in dark), the π–π^* absorption increases with a slight decrease in the

Table 2. Conditions for block copolymerization by chain extension from P(*n*BMA-*co*-MOAB)-Br MIs and block copolymer characterization.

no.	$[M]_0/[MI]_0$ [a)]	Time	Conversion	$\overline{M}_{n,th}$	$\overline{M}_n$ [c)]	PDI	*n*BMA [d)]	MOAB	S
		h	%	g · mol^{-1}	g · mol^{-1}		mol-%	mol-%	mol-%
BC-7	700	10.8	23.05	49 300	48 000	1.28	40.4	15.4	44.2
BC-8a	700	11.3	24.00	45 200	55 000	1.31	38.9	5.7	55.4
BC-8b [b)]	700	16.0	6.60	30 700	29 000	1.20	–	–	–
BC-9	700	11.8	27.40	46 000	52 500	1.16	48.0	3.2	48.2
BC-10	1 500	19.0	29.98	95 000	97 000	1.38	39.0	5.4	55.6
BC-11	450	26.5	26.7	33 000	40 000	1.29	35.3	14.8	50.0
BC-12	650	15.3	11.5	40 500	50 000	1.49	37.7	15.2	47.1

[a)] $[S]_0/[MI]_0/[CuBr]_0/[PMDETA]_0/[Sn(EH)_2]_0 = (450\text{–}1\,500){:}1{:}1{:}1{:}1$, MIs for BC-7–BC-12 were C-1–C-6, respectively; [b)] BC-8b without the presence of reducing agent $[Sn(EH)_2]$, and BC-7–BC-12 all at 90 °C in 50 vol.-% anisole; [c)] Molecular weights were determined from GPC traces with PS standard; [d)] Molar percentages were calculated by ^{1}H NMR.

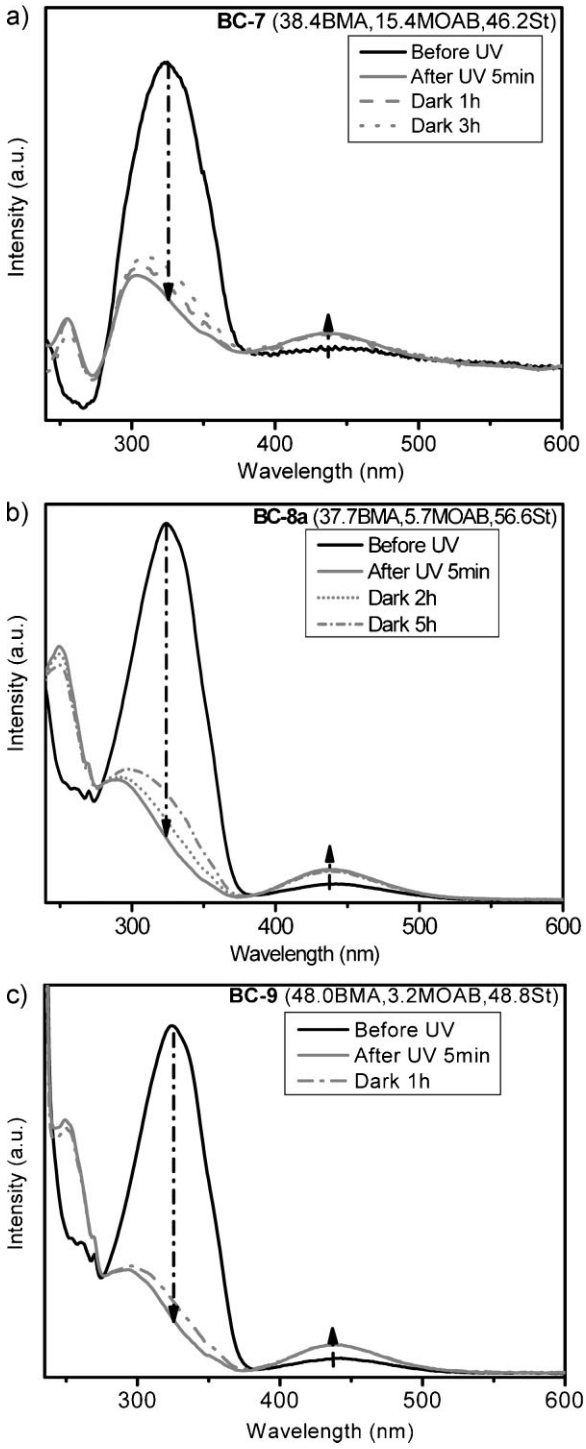

Figure 7. UV–Vis spectra of samples under UV 360 nm exposure before, after, and dark treatments with 0.01 mg · mL^{-1} $CHCl_3$ at room temperature for: (a) BC-7, (b) BC-8a, and (c) BC-9.

n–π^* absorption. This indicates that the photoisomerization of azobenzene undergoes a change from the *cis* to the *trans* state. The change of the absorption bands induced by UV irradiation is indicative of the photoisomerization of azobenzene from the *trans* to the *cis* state.

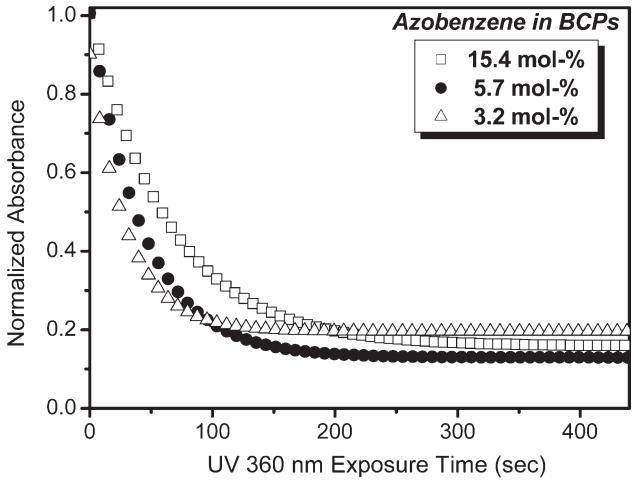

Figure 8. Photoisomerization kinetics for P(*n*BMA-*co*-MOAB)-*b*-PS BCPs with different azobenzene molar ratio (*trans* to *cis* measurements of *A(t)* at $\lambda = 325$ nm with 0.01 mg · mL^{-1} $CHCl_3$ at room temperature for BC-7, BC-8a, and BC-9 samples).

The kinetic of the photoisomerization was also measured from in situ UV–Vis measurements. The UV irradiation and visible light exposure time dependences of the absorbance at 325 nm for BC-7–BC-9 BCPs are shown in Figure 8. The photo-stationary state stage was reached in less than 3 min from *trans* to *cis* transition. The ordinate was normalized by the value of absorbance at time zero in the dark (A_0). The absorbance value at 325 nm exponentially decayed with increase in exposure time to visible light during the *trans* to *cis* transition. The experimental results were fitted for first-order isomerization reaction Equation (3):

$$\frac{A(t)}{A_0} = I \exp\left(-\frac{t}{\tau}\right) + I_0 \qquad (3)$$

Table 3. Photoisomerization of P(*n*BMA-*co*-MOAB)-*b*-PS di-BCPs.

	BC-7	BC-8a	BC-9
$\overline{M}_n$	52 700	65 900	52 500
Azo mol%	15.4	5.7	3.2
$\lambda_{\pi\to\pi^*}$ (nm)[a)]	325	326	325
$\lambda_{n\to\pi^*}$ (nm)	440	439	439
$\tau_{\pi\to\pi^*}$ (s)[b)]	64	43	30
$\tau_{n\to\pi^*}$ (s)	83	76	70
$A_{PSS}^{trans\to cis}/A_0$[c)]	0.84	0.89	0.80

[a)] $\lambda_{\pi\to\pi^*}$(nm): wavelength of *trans* absorption; $\lambda_{n\to\pi^*}$(nm): wavelength of *cis* absorption; [b)] $\tau_{\pi\to\pi^*}$(s): transition time from *trans* to *cis* conformation; $\tau_{n\to\pi^*}$(s): transition time from *cis* to *trans* conformation; [c)] photoisomerization efficiency.

Macromol. Chem. Phys. **2009**, *210*, 1484–1492

Macromolecular Journals
DOI: 10.1002/macp.200900195

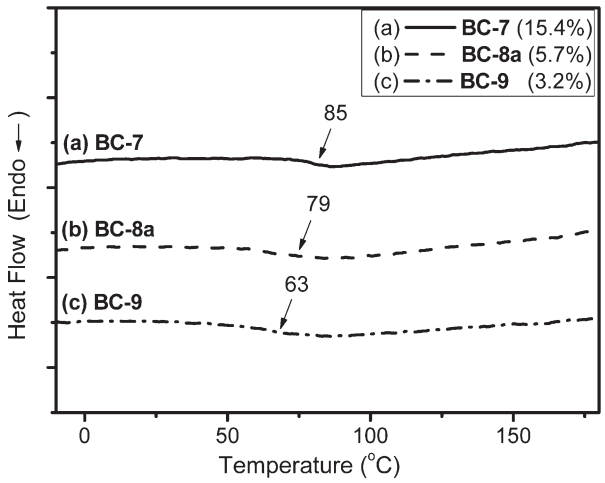

Figure 9. DSC thermograms (2nd run) of P(*n*BMA-*co*-MOAB)-*b*-PS BCPs with different azobenzene mol ratio: (a) BC-7 (15.4 mol-%), (b) BC-8a (5.7 mol-%), and (c) BC-9 (3.2 mol-%) [the samples (ca. 5–10 mg) were carried out for 1st run with 20 °C · min^{-1} for temperature up to 200 °C under $N_{2(g)}$; after quenching, then scanned for 2nd run up to 180 °C at 20 °C · min^{-1}].

The isomerization time, $\tau_{\pi\rightarrow\pi*}$ (*trans* to *cis* transition) and $\tau_{n\rightarrow\pi*}$ (*cis* to *trans*) are summarized in Table 3. The photoisomerization efficiency, for the *trans* to *cis* transition, $(A_{PSS}^{trans\rightarrow cis}/A_0)$ was near 80%. The *trans* to *cis* isomerization was faster (less than 1 min) than the *cis* to *trans* isomerization (70–80 s). The *trans* form of the azobenzene molecule was thermodynamically more stable and therefore the *cis* form obtained by photoisomerization returned to the *trans* form in the absence of the light for the P(*n*BMA-*co*-MOAB)-*b*-PS system.

A preliminary miscibility test of the BCPs was performed using DSC and X-ray reflectivity analyses. Figure 9 shows the conventional second run DSC thermograms of these BCPs with various molar ratios of azobenzene without UV radiation. A single T_g was observed, which suggested that these BCPs were not microphase separated. In Figure 10, thin film X-ray reflectivity results of the P(*n*BMA-*co*-MOAB)-*b*-PS BCP BC-7 showed that, in contrast to the profile without UV exposure, the reflectivity after UV exposure for 1 h possessed a breathing feature as a result of the beating of two frequencies that arose from an oscillation characteristic of the film thickness. Such oscillation of film thickness may come from the formation of island-hole structure at the initial state. The step height corresponds to the beating frequency. It is necessary that the di-BCP be microphase-separated to exhibit this surface topography which is indicative of LDOT. However, the precise morphology cannot be quantified due to the low electron density difference between PS and P*n*BMA blocks for hard X-ray. Film studies of temperature and UV-induced LDOT behavior by SANS are currently being carried out to further understand the relationships of the physical property changes, such as the solubility parameter, morphology, and refractive index to the photo-addressable composition in polymer chain to precisely determine the location of the microphase separation transition in the phase diagram.

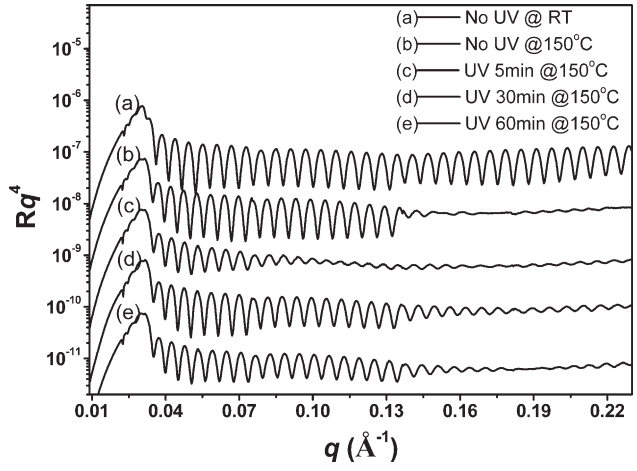

Figure 10. X-ray reflectivity profiles of P(*n*BMA-*co*-MOAB)-*b*-PS BCP BC-7 thin film under UV light with a wavelength of 365 nm and an intensity of 5 mW · cm^{-2} at 150 °C for different exposure times. The copolymer film was pre-annealed at 150 °C for 24 h under vacuum.

Conclusion

A series of P(*n*BMA-*co*-MOAB)-*b*-PS di-BCPs with a photoisomerizable azobenzene moiety were successfully synthesized. Preparation of the P(*n*BMA-*co*-MOAB)-Br MI by ARGET ATRP showed that variation of the concentration of MOAB in the feed had no significant influence on polymerization rate. Faster incorporation of MOAB than BMA resulted in weak gradient distribution of *n*BMA and MOAB in the copolymer. The rate of polymerization for the ATRP chain extension with styrene in the presence of reducing agent was strongly accelerated (ca. 10-fold), providing low polydispersity P(*n*BMA-*co*-MOAB)-*b*-PS di-BCPs. $\overline{M}_w/\overline{M}_n = 1.16–1.49$, and $\overline{M}_n$ values are in good agreement with the calculated values. These results showed that well-controlled BCPs with styrene were prepared. Photoisomerization of the P(*n*BMA-*co*-MOAB)-*b*-PS BCPs was studied in $CHCl_3$. The photoisomerization efficiency for the *trans* to *cis* transition $(A_{PSS}^{trans\rightarrow cis}/A_0)$ was about 80%, with the *trans* to *cis* isomerization time being shorter than *cis* to *trans*. In the P(*n*BMA-*co*-MOAB)-*b*-PS system, the *cis* form returned to the *trans* form in the absence of light, since the *trans* form of the azobenzene molecule is thermodynamically more stable. The self-assembly of the diblock polymer in bulk state and the UV-induced LDOT behavior variations will be presented in a future publication.

Acknowledgements: This research was financially supported by the *Department of Energy, Office of Basic Energy Science* (*DE FG02 02ER45998).* C.-F. Huang acknowledges *National Science Council* and *National Chiao Tung University* (NSC-096-2120-M-009-009 and NSC-096-2917-I-564-131) for the postdoctoral fellowship.

Received: May 3, 2009; Published online: August 14, 2009; DOI: 10.1002/macp.200900195

Keywords: ARGET ATRP; azobenzene; block copolymers; reflectivity; X-ray

[1] F. S. Bates, *Science* **1991**, *251*, 898.
[2] E. L. Thomas, D. M. Anderson, C. S. Henkee, D. Hoffman, *Nature* **1988**, *334*, 598.
[3] L. Leibler, *Macromolecules* **1980**, *13*, 1602.
[4] M. W. Matsen, F. S. Bates, *Macromolecules* **1996**, *29*, 1091.
[5] J. Dudowicz, K. F. Freed, *Macromolecules* **2000**, *33*, 5292.
[6] T. Hashimoto, H. Hasegawa, H. Katayama, M. Kamigaito, M. Sawamoto, *Macromolecules* **1997**, *30*, 6819.
[7] A. V. G. Ruzette, P. Banerjee, A. M. Mayes, M. Pollard, T. P. Russell, R. Jerome, T. Slawecki, R. Hjelm, P. Thiyagarajan, *Macromolecules* **1998**, *31*, 8509.
[8] A. V. G. Ruzette, P. Banerjee, A. M. Mayes, T. P. Russell, *J. Chem. Phys.* **2001**, *114*, 8205.
[9] A. V. G. Ruzette, A. M. Mayes, M. Pollard, T. P. Russell, B. Hammouda, *Macromolecules* **2003**, *36*, 3351.
[10] D. Y. Ryu, U. Jeong, J. K. Kim, T. R. Russell, *Nat. Mater.* **2002**, *1*, 114.
[11] D. Y. Ryu, D. H. Lee, U. Jeong, S. H. Yun, S. Park, K. Kwon, B. H. Sohn, T. Chang, J. K. Kim, T. P. Russell, *Macromolecules* **2004**, *37*, 3717.
[12] D. Y. Ryu, M. S. Park, S. H. Chae, J. Jang, J. K. Kim, T. P. Russell, *Macromolecules* **2002**, *35*, 8676.
[13] T. E. Karis, T. P. Russell, Y. Gallot, A. M. Mayes, *Macromolecules* **1995**, *28*, 1129.
[14] M. Pollard, T. P. Russell, A. V. Ruzette, A. M. Mayes, Y. Gallot, *Macromolecules* **1998**, *31*, 6493.
[15] D. Y. Ryu, D. J. Lee, J. K. Kim, K. A. Lavery, T. P. Russell, Y. S. Han, B. S. Seong, C. H. Lee, P. Thiyagarajan, *Phys. Rev. Lett.* **2003**, *90*, 235501.
[16] D. H. Lee, H. J. Kim, J. K. Kim, *Macromol. Symp.* **2006**, *240*, 123.
[17] T. Seki, *Bull. Chem. Soc. Jpn.* **2007**, *80*, 2084.
[18] H. Nakanishi, M. Satoh, T. Norisuye, Q. Tran-Cong-Miyata, *Macromolecules* **2004**, *37*, 8495.
[19] H. Nishioka, K. Kida, O. Yano, Q. Tran-Cong, *Macromolecules* **2000**, *33*, 4301.
[20] Q. Tran-Cong-Miyata, J. Kawai, K. Endoh, *Chaos* **1999**, *9*, 298.
[21] Q. Tran-Cong-Miyata, S. Nishigami, T. Ito, S. Komatsu, T. Norisuye, *Nat. Mater.* **2004**, *3*, 448.
[22] O. Kuksenok, R. D. M. Travasso, A. C. Balazs, *Phys. Rev. E* **2006**, *74*.
[23] R. D. M. Travasso, O. Kuksenok, A. C. Balazs, *Langmuir* **2006**, *22*, 2620.
[24] K. Ichimura, *Chem. Rev.* **2000**, *100*, 1847.
[25] A. Natansohn, P. Rochon, *Chem. Rev.* **2002**, *102*, 4139.
[26] S. K. Yesodha, C. K. S. Pillai, N. Tsutsumi, *Prog. Polym. Sci.* **2004**, *29*, 45.
[27] L. Cui, X. Tong, X. H. Yan, G. J. Liu, Y. Zhao, *Macromolecules* **2004**, *37*, 7097.
[28] J. Li, K. Kamata, M. Komura, T. Yamada, H. Yoshida, T. Iyoda, *Macromolecules* **2007**, *40*, 8125.
[29] Y. Q. Tian, K. Watanabe, X. X. Kong, J. Abe, T. Iyoda, *Macromolecules* **2002**, *35*, 3739.
[30] H. F. Yu, S. Asaoka, A. Shishido, T. Iyoda, T. Ikeda, *Small* **2007**, *3*, 768.
[31] H. F. Yu, T. Iyoda, T. Ikeda, *J. Am. Chem. Soc.* **2006**, *128*, 11010.
[32] S. Kadota, K. Aoki, S. Nagano, T. Seki, *J. Am. Chem. Soc.* **2005**, *127*, 8266.
[33] J. S. Wang, K. Matyjaszewski, *Macromolecules* **1995**, *28*, 7901.
[34] T. E. Patten, J. H. Xia, T. Abernathy, K. Matyjaszewski, *Science* **1996**, *272*, 866.
[35] K. Matyjaszewski, J. Xia, *Chem. Rev.* **2001**, *101*, 2921.
[36] W. Jakubowski, K. Matyjaszewski, *Angew. Chem., Int. Ed.* **2006**, *45*, 4482.
[37] K. Matyjaszewski, W. Jakubowski, K. Min, W. Tang, J. Y. Huang, W. A. Braunecker, N. V. Tsarevsky, *Proc. Natl. Acad. Sci. USA* **2006**, *103*, 15309.
[38] N. V. Tsarevsky, K. Matyjaszewski, *Chem. Rev.* **2007**, *107*, 2270.
[39] K. Min, H. Gao, K. Matyjaszewski, *J. Am. Chem. Soc.* **2005**, *127*, 3825.
[40] W. Jakubowski, K. Min, K. Matyjaszewski, *Macromolecules* **2006**, *39*, 39.
[41] J. H. Xia, S. G. Gaynor, K. Matyjaszewski, *Macromolecules* **1998**, *31*, 5958.
[42] H. I. Lee, J. Pietrasik, K. Matyjaszewski, *Macromolecules* **2006**, *39*, 3914.
[43] R. Solaro, A. Altomare, F. Ciardelli, *Eur. Polym. J.* **1990**, *26*, 649.
[44] J. P. Kennedy, T. Kelen, F. Tudos, *J. Polym. Sci., Part A: Polym. Chem.* **1975**, *13*, 2277.
[45] A. S. Brar, M. Thiyagarajan, *J. Polym. Sci., Part A: Polym. Chem.* **1999**, *37*, 3179.
[46] A. S. Brar, M. Thiyagarajan, *J. Appl. Polym. Sci.* **1999**, *74*, 3016.
[47] A. S. Brar, M. Thiyagarajan, *Eur. Polym. J.* **2001**, *37*, 507.
[48] S. V. Arehart, K. Matyjaszewski, *Macromolecules* **1999**, *32*, 2221.
[49] M. J. Ziegler, K. Matyjaszewski, *Macromolecules* **2001**, *34*, 415.
[50] K. Matyjaszewski, M. J. Ziegler, S. V. Arehart, D. Greszta, T. Pakula, *J. Phys. Org. Chem.* **2000**, *13*, 775.
[51] K. Matyjaszewski, H.-J. Paik, P. Zhou, S. J. Diamanti, *Macromolecules* **2001**, *34*, 5125.
[52] K. Matyjaszewski, S. G. Gaynor, *Macromolecules* **1997**, *30*, 7042.
[53] K. Matyjaszewski, *Macromolecules* **2002**, *35*, 6773.

DOI: 10.1002/macp.200900195